Kolb, H.-A., Läuger, P., & Bamberg, E. (1975) *J. Membr. Biol. 20*, 133-154.
Kukolich, S. G. (1969) *J. Chem. Phys. 51*, 358-360.
Nicholson, L. K., Moll, F., Mixon, T. E., LoGrasso, P. V., Lay, J. C., & Cross, T. A. (1987) *Biochemistry 26*, 6621-6626.
Pauls, K. P., MacKay, A. L., Soderman, O., Bloom, M., Tanjea, A. K., & Hodges, R. S. (1985) *Eur. Biophys. J. 12*, 1-11.
Poupko, R., Luz, Z., Vega, A. J., & Zimmermann, H. (1987) *J. Chem. Phys. 86*, 5358-5364.
Prasad, B. V. V., & Chandrasekaran, R. (1977) *Int. J. Pept. Protein Res. 10*, 129-138.
Prasad, K. U., Trapane, T. L., Busath, D., Szabo, G., & Urry, D. W. (1982) *Int. J. Pept. Protein Res. 19*, 162-171.
Pschorn, O., & Spiess, H. W. (1980) *J. Magn. Reson. 39*, 217-228.
Sarges, R., & Witkop, B. (1965) *J. Am. Chem. Soc. 87*, 2027-2030.
Seelig, J. (1977) *Q. Rev. Biophys. 10*, 353-418.
Seelig, J. (1978) *Biochim. Biophys. Acta 515*, 105-140.
Seelig, J., Borle, F., & Cross, T. A. (1985) *Biochim. Biophys. Acta 814*, 195-198.
Spiess, H. W., & Sillescu, H. (1981) *J. Magn. Reson. 42*, 381-389.
Thadeus, P., Krishner, L. C., & Loubser, J. (1964) *J. Chem. Phys. 40*, 257-273.
Urry, D. W. (1971) *Proc. Natl. Acad. Sci. U.S.A. 68*, 672-676.
Urry, D. W., Goodall, M. C., Glickson, J. D., & Mayers, D. F. (1971) *Proc. Natl. Acad. Sci. U.S.A. 68*, 1907-1911.
Urry, D. W., Trapane, T. L., Romanowski, S., Bradley, R. J., & Prasad, K. U. (1983) *Int. J. Pept. Protein Res. 21*, 16-23.
Veatch, W. R., Fossel, E. T., & Blout, E. R. (1974) *Biochemistry 13*, 5249-5256.
Veatch, W. R., Mathies, R., Eisenberg, M., & Stryer, L. (1975) *J. Mol. Biol. 99*, 75-92.
Vega, A. J., & Luz, Z. (1987) *J. Chem. Phys. 86*, 1803-1813.
Venkatachalam, C. M., & Urry, D. W. (1983) *J. Comput. Chem. 4*, 461-469.
Wittebort, R. J., Olejniczak, E. T., & Griffin, R. G. (1987) *J. Chem. Phys. 86*, 5411-5420.
Zingsheim, H. P., & Neher, E. (1974) *Biophys. Chem. 2*, 197-207.

Resonance Raman Characterization of *Chromatium vinosum* Cytochrome *c'*. Effect of pH and Comparison of Equilibrium and Photolyzed Carbon Monoxide Species†

J. D. Hobbs,‡ R. W. Larsen,‡ T. E. Meyer,§ J. H. Hazzard,§ M. A. Cusanovich,§ and M. R. Ondrias*,‡

Department of Chemistry, University of New Mexico, Albuquerque, New Mexico 87131, and Department of Biochemistry, University of Arizona, Tucson, Arizona 85721

Received May 23, 1989; Revised Manuscript Received January 2, 1990

ABSTRACT: Resonance Raman spectra of *Chromatium vinosum* cytochrome *c'* have been obtained for the five pH-dependent states of the protein [i.e., types I (pH 7), II (pH 10), and III (pH 12) of the ferric protein and type a (pH 7) and type n (pH 12) of the ferrous protein]. The raman spectra of type II and type a are consistent with those of high-spin, 5-coordinate heme proteins, such as deoxyhemoglobin, while spectra of type III and type n correspond more closely to those of low-spin, ferric and ferrous cytochrome *c*, respectively. Spectra of the CO-bound equilibrium species qualitatively resemble those of carbon monoxy human HbA. However, both the Fe–C and C=O stretching modes of the ligated species exhibit pH-dependent frequency shifts. Our data also indicate that CO photolysis is much more efficient at pH 7 than at pH 12. Moreover, the spectra of the photolytic transients suggest that unique, high-spin species are formed subsequent to CO photolysis from both type a and type n species.

The bacterial cytochromes *c'* are a general class of mono- and diheme proteins found throughout photosynthetic and dentrifying bacteria (Bartsch, 1978; Meyer & Kamen, 1982). The cytochrome *c'* isolated from the purple photosynthetic bacterium *Chromatium vinosum* is a dimeric heme protein consisting of two identical subunits. Unlike most *c*-type heme proteins, ferrous cytochrome *c'* derived from *C. vinosum* reversibly binds carbon monoxide in its reduced form, but reacts with oxygen and nitric oxide irreversibly (Cusanovich, 1971; Kennel et al., 1972). The ferric form of this protein also binds cyanide (CN^-) and ethyl isocyanide with an affinity that is lower than that found for either horse heart cytochrome *c* or myoglobin (Kassner et al., 1985; Rubinow & Kassner, 1984).

The cytochromes *c'* exhibit several distinctive spectroscopic characteristics. In particular, the variations in their absorption spectra with pH have been of considerable interest. Ferric cytochromes *c'* exhibit three distinct types of UV-visible absorption and EPR spectra, depending upon the pH (Imai et al., 1969; Maltempo, 1975). In the UV-visible absorption, these have been labeled type I (pH 7), type II (pH 10), and

† This work was performed at the University of New Mexico and was supported by NIH Grants GM33330 (to M.R.O.) and GM21277 (to M.A.C.).
‡ University of New Mexico.
§ University of Arizona.

0006-2960/90/0429-4166$02.50/0

type III (pH 12). The first two are predominantly high-spin, and the third is low-spin. The spectrum of the reduced form of cytochrome *c'* is anomalous, relative to other *c*-type cytochromes, and is labeled type a in the pH region where the spectrum of the oxidized form is either type I or type II. It is, however, converted to a "normal," low-spin spectrum (type n) at more alkaline pH (>11.5). The conversions between forms I and II and between forms II and III have been shown to be reversible (Imai et al., 1969). Addition of propanol, or a large change in ionic strength, has also been found to produce a direct conversion between types I and III (Imai et al., 1969). Thus, it is apparent that environmental perturbations of protein tertiary structure result in systematic changes at the heme active sites of cytochromes *c'*. These properties make this class of heme protein amenable for the study of ligand and protein matrix effects upon the heme site.

Several studies (Doyle et al., 1986; Cusanovich & Gibson, 1973) have also demonstrated unique ligand binding properties in the cytochrome *c'* isolated from *C. vinosum*. Specifically, it has been reported that the carbon monoxide binding to the heme is cooperative with a large endothermic heat of ligation. Most interestingly, there is direct evidence of a CO-linked dimer–monomer dissociation equilibrium. Gel filtration studies have confirmed that, at micromolar concentrations (0.5–50 μM), the physiological state is a tightly associated dimer in both the oxidized and reduced forms of the cytochrome. Additions of saturating concentrations of CO produce dissociation of reduced dimers (Doyle et al., 1986). Further, the kinetics of carbon monoxide binding are complex and involve at least three separate second-order processes which may originate in the ligand-linked dissociation reaction (Doyle et al., 1986).

In this study, transient resonance Raman spectroscopy has been employed to further characterize the equilibrium and dynamic structures of the heme active site and protein environment as they relate to the pH-induced absorption changes and ligand binding properties of this enzyme. Resonance Raman spectroscopy has been shown to yield a variety of information on the porphyrin macrocycle and iron ion which constitute the active site of many aqueous as well as membrane-bound enzymes. These include iron oxidation and spin state, porphyrin peripheral substituents, and proximal and distal heme ligand geometry (Spiro, 1983; Babcock, 1980; Yu & Kerr, 1988). Previous Raman investigations of the cytochrome *c'* centered upon the steady-state characteristics of the enzyme as they pertain to varying pH (Streakas & Spiro, 1974; Kitagawa et al., 1977). Our data expand upon these studies by presenting Soret-enhanced low-frequency (200–600 cm^{-1}) spectra as well as ligand binding and dynamic information for these covalently bound hemes.

Materials and Methods

Chromatium vinosum cytochrome *c'* was prepared by the method of Bartsch (1971), lyophilized, and stored at −10 °C. The Raman samples were prepared by dissolving ~0.5 mg of lyophilized protein in ~200 μL of 0.1 M phosphate buffer at the appropriate pH. The final heme concentration of the Raman samples was ~100 μM. Both sample pH and absorption spectra were monitored before and after the Raman experiments.

The fully reduced protein was prepared by degassing the dissolved sample in an anaerobic optical cell. Solid sodium dithionite was then added to the cell under a positive N_2 atmosphere. Reduction was verified by monitoring the absorption spectrum on an HP8452 diode array UV/VIS spectrophotometer. The CO-ligated species were prepared by flushing the fully reduced samples with ~60 mmHg of CO scrubbed by KOH to remove CO_2. After four cycles of vacuum/CO, a final CO atmosphere of 150 mmHg was applied. Samples were then incubated for 45 min to 1 h at ~10 °C prior to use. During the Raman experiment, the samples were cooled to ~15 °C by a stream of refrigerated N_2 gas. The CN^--bound ferric complex was prepared at pH 7.0 by the method of Kassner et al. (1985).

Resonance Raman spectra were obtained by using a Molectron UV-24 nitrogen-pumped dye laser (tunable range from 335 to 800 nm) using back-scattering geometry. Laser power density at the sample was varied from 10 to 150 mJ/cm^2 pulse using either cylindrical or spherical focusing optics. Defocused cylindrical optics were required in order to obtain spectra of the CO-bound species, without significant CO photolysis. The scattered light was collected and dispersed with a Spex 1403 double monochromator. The data were stored and processed on a Spex DM3000 XT computer.

The CO–protein complex was prepared for the infrared experiments by the addition of a solution of sodium dithionite to a CO-saturated solution of oxidized protein that had been previously concentrated to 3–4 mM in heme. The final concentration of dithionite was 20–30 mM in a 100 mM phosphate buffer. The sample was transferred to the infrared cell in an argon-filled glovebag. Infrared spectra were obtained with a Nicolet 5PC FTIR operating at 2 cm^{-1} resolution and averaging 100 scans. Sample pH was adjusted by dilution of the concentrated protein into buffer of the appropriate pH and reconcentration in a stirred cell. Gaussian deconvolutions of the C–O stretching band were performed as previously described (Shimada & Caughey, 1982).

Results

High-Frequency Spectra of Ferric and Ferrous Species. Soret excitations (406–413 nm) enhance polarized and depolarized Raman bands corresponding to in-plane porphyrin ring vibrations (Spiro, 1983). These bands are most prominent in the high-frequency (1100–1700 cm^{-1}) region of the spectrum and have been found to be highly reliable indicators of the heme environment, especially the oxidation and spin state of the iron ion. Several bands in the low-frequency spectrum (<1000 cm^{-1}) are associated with either ligand–metal vibrations or out-of-plane porphyrin skeletal modes.

Figures 1–3 present spectra of type I, II, and III and type a and n species. Our data are completely consistent with previously published results for a monomeric species of cytochrome *c'* (Strekas & Spiro, 1974). The type II species of ferric cytochrome *c'* exhibits positions for ν_3 (1493 cm^{-1}) and ν_{10} (1629 cm^{-1}) which are more characteristic of a high-spin ferric heme. On the other hand, the high-frequency spectrum of the type I form is anomalous in that the spin state sensitive bands, ν_2(1580 cm^{-1}), ν_3(1502 cm^{-1}), and ν_{10}(1637 cm^{-1}), have frequencies intermediate between those of low-spin 6-coordinate hemes and the high-spin, pentacoordinate hemes. EPR data are consistent with a high-spin species at pH 10 (type II), whereas those at pH 7 are conjectured to represent a single species which is a quantum mechanical admixture of high ($S = {}^5/_2$) and intermediate ($S = {}^3/_2$) spin states (Maltempo, 1975; Maltempo et al., 1974). At pH values >11.5, both the Raman and EPR data suggest the formation of a low-spin ferric state consistent with the binding of a strong-field ligand, such as histidyl imidazole nitrogen. This can be observed in Figure 1 by shifts in ν_4 to 1377 cm^{-1}, ν_2 to 1590 cm^{-1}, ν_3 to 1506 cm^{-1}, and ν_{10} to 1639 cm^{-1}. Thus, the Raman spectra of the type III cytochrome *c'* from *C. vinosum* correspond closely with spectra from other low-spin heme proteins, such as ferric-

Table I: Resonance Raman Frequencies (in cm^{-1}) for Cytochrome *c'* under a Variety of pH and Ligand Conditions

	Fe(III)				Fe(II)				
	pH 7.0	pH 10.0	pH 12.0	-CN	pH 7.0	pH 12.0	-CN	pH 7.0, -CO	pH 12.0, -CO
ν_4	1371	1371	1377	1372	1352	1358	1356	1371	1370
ν_3	1502	1493	1506	1508	1469	1488	1471	1467	1470
ν_2	1580	1580	1590	1589	1577	1592	1588	1591	1592
ν_{10}	1637	1629	1639						
ν_{Fe-His}					231	232			
ν_{Fe-CO}								492	496

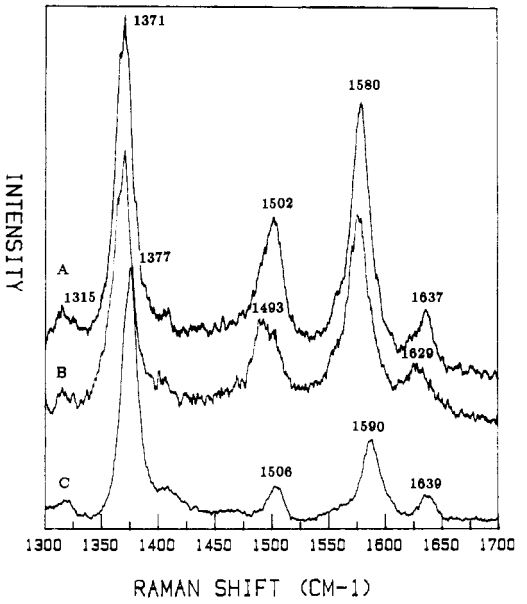

FIGURE 1: High-frequency Raman spectra of ferricytochrome *c'* from *C. vinosum* obtained by using Soret enhancement (406 nm): (A) at pH 7.0 (type I); (B) at pH 10.0 (type II); and (C) at pH 12.0 (type III). All samples were in 0.1 M phosphate buffer, and the pH was adjusted by using concentrated HCl or NaOH. Spectra are the unsmoothed sum of three scans with an average laser power of ~5 mW at 10Hz. The spectral band-pass was 7–9 cm^{-1} for all spectra.

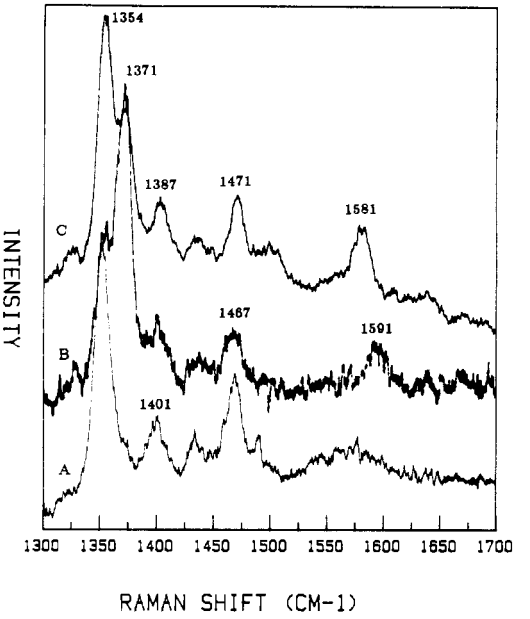

FIGURE 2: High-frequency Raman spectra of (A) dithionite-reduced, (B) CO-ligated, and (C) 10-ns photolyzed cytochrome *c'* at pH 7.0. CO-ligated Raman samples were prepared as described under Materials and Methods. The spectrum of the CO-ligated sample was obtained by using low (~4 mW) laser power (λ = 406 nm) and by defocusing the laser beam on the sample cuvette. CO photolysis data were obtained by increasing the laser power (to ~8 mW) and focusing the laser beam directly on the sample cuvette.

ytochrome *c* (ν_2, 1374; ν_3, 1502; ν_{10}, 1636 cm^{-1}) and cyanoHRP (ν_2, 1375; ν_3, 1497; ν_{10}, 1642 cm^{-1}).

Another low-spin species was generated by binding CN^- to the ferric protein (data not shown). Spectra of this species strongly resemble those of the ferric species at pH 12.0. The spin state sensitive bands ν_2 and ν_3 shift to 1589 and 1508 cm^{-1}, respectively. However, ν_4, which is sensitive to the electron density of the porphyrin π^* molecular orbital, remains virtually unperturbed. Small additions of $Na_2S_2O_4$ produce the ferrous, CN^--bound species which can be distinguished both by a shift in ν_4 to 1356 cm^{-1} due to reduction of the iron ion and by the presence of a "low-spin" ν_2 (1588 cm^{-1}) (data not shown).

The raman spectra of the reduced forms [types a (pH 7) and n (pH 12)] generally resemble those of deoxyhemoglobin and ferrous cytochrome *c*, respectively. At pH 7, the positions ν_4(1352), ν_3(1469), and ν_2(~1577) cm^{-1} are characteristic of a high-spin heme. However, the low relative intensity of ν_2 is quite unusual for a ferrous, high-spin heme. Increasing the pH to >11.5 produces changes in the Raman spectra (see Table I) indicative of the formation of a low-spin species. This is presumably due to the binding of an endogenous ligand to form the hexacoordinate complex. Interestingly, the relative intensity of ν_2 for the type n species is quite typical of a low-spin heme.

CO-Ligated and Photolyzed Species. The high-frequency Raman spectra of the CO-liganded and 10-ns photolyzed cytochromes *c'* are shown in Figures 2 and 3. Shifts in ν_4 to high frequency (1371 cm^{-1}) relative to that of the reduced species (1351 cm^{-1}) at pH 7 are indicative of a decrease in

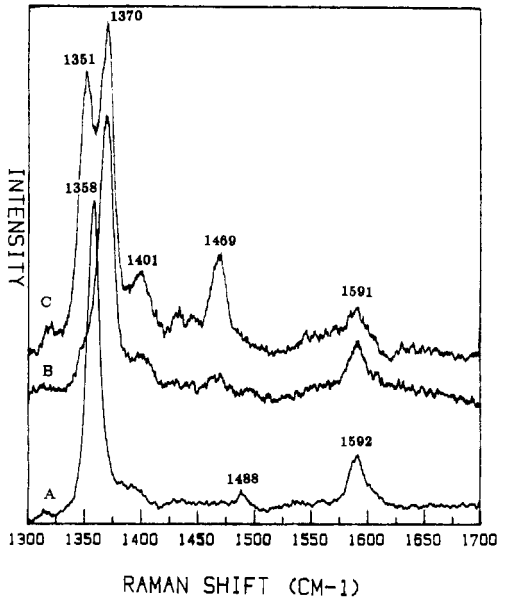

FIGURE 3: High-frequency Raman spectra of (A) dithionite-reduced, (B) CO-ligated, and (C) 10-ns photolyzed cytochrome *c'* at pH 12.0. Experimental conditions were as described in Figure 2.

the electron density of the π^* antibonding orbitals or the porphyrin macrocycle by back-bonding to the CO through the iron d_π orbitals. The modes (ν_2) appearing at 1590 cm^{-1} in the pH 7 sample and at 1592 cm^{-1} in the pH 12 sample

Table II

	Raman Modes for Ferroheme Proteins (in cm^{-1})						
	HbA[a]	Mb[b]	CHP[c]	*c'* (pH 7)	*c'* (pH 12)	CCP (pH 7)[d]	CCP (pH 8.3)[d]
ν_4	1357	1355	1354	1352	1358	1355	1354
ν_3	1473	1472	1469	1469	1488	1472	1472
ν_2	1568		1575	1577	1592	1565	1565
ν_{10}	1604	1604	1605				1603
ν_{Fe-His}	215[f]	220[f]		231	232	248	227

	Raman Modes for CO-Ligated Heme Proteins (in cm^{-1})					
	HbA	Mb	CCP	CHP[e]	*c'* (pH 7)	*c'* (pH 12)
ν_4	1372	1372	1372	1371	1371	1370
ν_3	1471	1472	1472	1468	1467	1469
ν_2	1586	1587	1580	1590	1591	1592
ν_{Fe-CO}[g]	507		505–510	518	492	496
$\nu_{C=O}$[g]	1951	1944	1922		1978	1972

[a] Felton & Yu (1983). [b] Felton & Yu (1983). [c] Ondrias et al. (1984). [d] Dasgupta et al. (1989). [e] Gaul et al. (1987). [f] Kitagawa (1988). [g] Tabulated in Li and Spiro (1988).

Table III: Infrared Frequencies (in cm^{-1}) for Cytochrome *c'* from Spectral Deconvolution

band location (cm^{-1})	relative intensity (cm^{-1})	
	pH 7	pH 12
1985 ± 0.05		
1979	16 ± 5	0
1967	31	44
1954	9	11

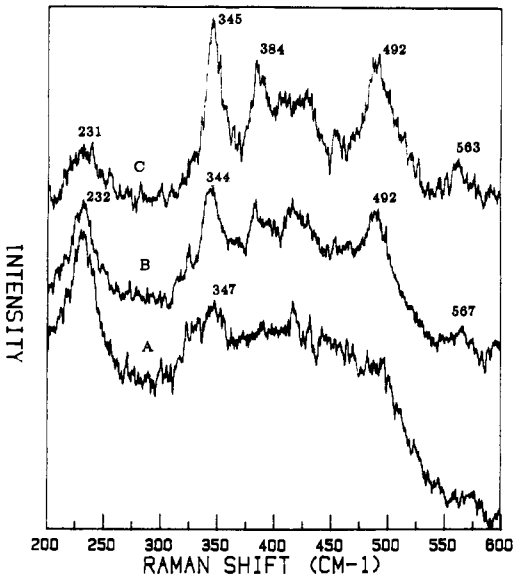

FIGURE 4: Low-frequency Raman spectra of (A) dithionite-reduced, (B) 10-ns CO-photolyzed, and (C) CO-ligated cytochrome *c'* at pH 7.0. Experimental conditions were the same as those for previous figures.

(Figure 3) are consistent with formation of a low-spin iron–porphyrin complex upon CO binding. The high-frequency Raman bands observed in the cytochrome *c'*–CO complex correspond well with those reported for CO complexes of Hb, Mb, and cytochrome *c* peroxidase (see Table II).

CO photolysis from cytochrome *c'* initially generates a 5-coordinate high-spin ferrous species under either pH 7.0 or pH 12.0 conditions. This is most evident in the growth of the relative intensity of ν_4 at ~1355 cm^{-1} with increasing pulse energies. However, it is clear that both the net quantum yield for ligand photolysis and the transient heme species created are quite pH dependent. Figures 2 and 3 demonstrate that the net quantum yield for CO photolysis with 10-ns photolysis pulses (~0.2 mJ/pulse) is substantially greater for the pH 7.0 sample than for the pH 12.0 sample. Indeed, at pH 7.0, some photolysis was apparent even at the lowest laser energy

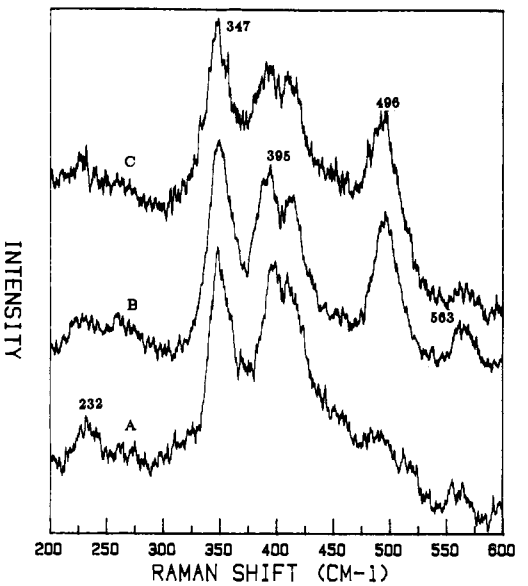

FIGURE 5: Low-frequency Raman spectra of (A) dithionite-reduced, (B) CO-ligated, and (C) 10-ns CO-photolyzed cytochrome *c'* at pH 12.0. Experimental conditions were the same as those for previous figures.

used (~0.05 mJ/pulse) (see Figure 2). The spectra of the photolytic transient heme species are quite distinct from those of the analogous equilibrium ferrous species at either pH.

Low-Frequency Spectra. Modes in the 200–800 cm^{-1} range are particularly informative with regard to heme out-of-plane deformations, the vibrations of peripheral substituents, and axial ligands (Spiro, 1983). The Raman spectrum obtained using Soret excitation of ferrous cytochrome *c'* at pH 12 (Figure 5) strongly resembles that of ferrous cytochrome *c* where the most intense grouping of heme modes occurs in the 325–425 cm^{-1} region of the spectrum. However, the ferrous high-spin form of the protein (pH 7) yields a unique low-frequency spectrum (Figure 4). We have tentatively assigned the Fe–histidine stretching frequency at 232 cm^{-1} in this species. This mode is most prominent in spectra of the pentacoordinate, type a form of ferrous cytochrome *c'*. The weak band at ~230 cm^{-1} in Figure 4A comes from the photolyzed fraction of the sample. The position of this band is intermediate between those found for deoxyhemoglobins and deoxymyoglobins (<220 cm^{-1}) and those observed in HPR and CCP (>240 cm^{-1}). The dramatic decrease in the intensity of the ~230 cm^{-1} band upon the protein "a" to "n" transition is also consistent with its assignment as an Fe–His mode (see Discussion). Other low-frequency heme modes are also drastically affected by the pH-induced "a" to "n" transition. The relative

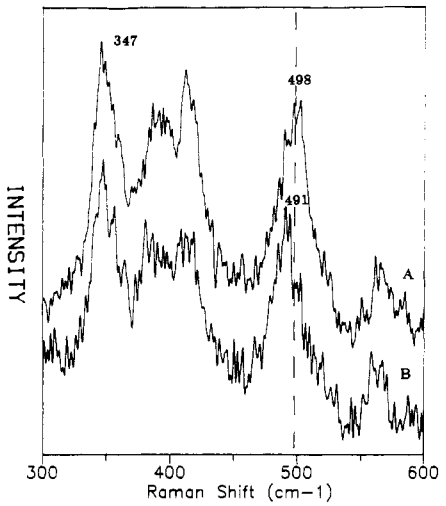

FIGURE 6: Low-frequency Raman spectra of (A) ^{12}CO-ligated and (B) ^{13}CO-ligated cytochrome *c'* at pH 12.0. Obtained under low laser power conditions (as described previously).

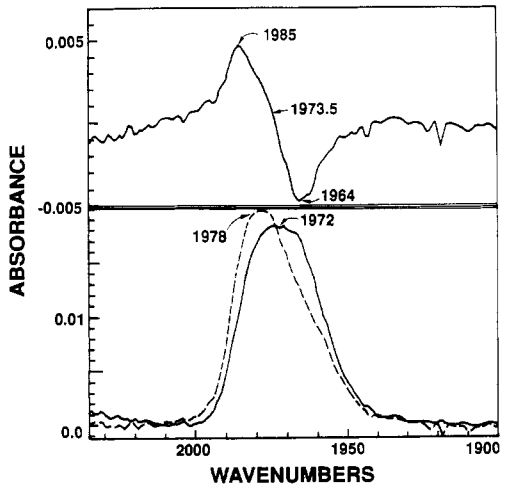

FIGURE 7: (Lower panel) FTIR spectra of the CO complex of *C. vinosum* cytochrome *c'* at pH 7 and 12. Solution conditions are described in the text. Both spectra were obtained at 25 °C using a thermostated cell with CaF_2 windows and a path length of 0.005 cm. Integrated areas of the bands have been normalized. (Upper panel) FTIR difference spectrum, pH 7 minus pH 12.

intensities of heme modes appearing at 348, 399, and 410 cm^{-1} are significantly increased. This alteration of the heme may be due to protein conformational effects or more direct perturbations of the heme geometry. We assign the 492 cm^{-1} (pH 7) and 496 cm^{-1} (pH 12) bands in the low-frequency CO-ligated spectra (Figures 4 and 5) to the Fe–C stretching frequency based upon their approximate 5 cm^{-1} shift to lower frequency for the ^{13}CO vs ^{12}CO species (see Figure 6).

Figure 7 demonstrates that the carbon–oxygen stretch frequency of CO bound to *Chromatium* cytochrome *c'* is sensitive to pH in terms of band shape and location of the absorbance maximum. The shift in intensity in the transition from pH 7 to pH 12 is approximately 20 cm^{-1}, from 1985 to 1964 cm^{-1}. The C–O band is not symmetric and can be deconvoluted to reveal four bands at neutrality and three bands at pH 12. The difference spectrum is apparently due to a shift in the 1985 cm^{-1} band to 1967 cm^{-1} (see Figure 8).

Addition of CO to the dithionite-reduced samples produced bands at 492 and 496 cm^{-1} in the low-frequency spectra at pH 7 and pH 12, respectively. These bands are assigned as the Fe-C stretching modes based upon two observations: (1) The intensity of these bands could be reduced by increasing the

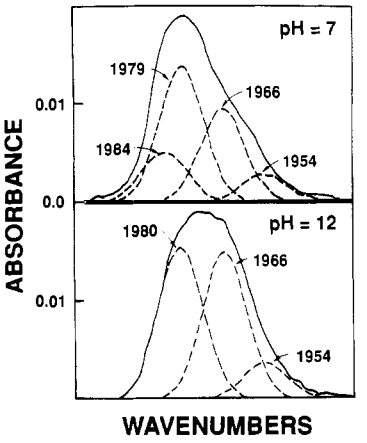

FIGURE 8: FTIR spectrum of cytochrome *c'* at pH 7 (upper panel) and pH 12.0 (lower panel). The theoretical Gaussian bands used in the spectral deconvolution are shown beneath the experimental data. Approximate theoretical band parameters are given in Table III.

laser flux and thus increasing the degree of ligand photolysis. (2) ^{13}CO isotopic substitution produced an approximate 5 cm^{-1} downshift in the 496 cm^{-1} band. A weaker band at ~565 cm^{-1} also appears as a consequence of CO binding. By analogy to spectra of other CO-ligated heme proteins, this band might be assigned as the Fe–C–O bending mode. However, in view of its apparent insensitivity to isotropic substitution (see Figure 7), this assignment would be quite sepculative.

Discussion

Amino acid sequence data from a variety of cytochromes *c'* (Ambler et al., 1981) and X-ray crystallographic data of the cytochrome *c'* isolated from *Rhodospirillum molischianum* (Weber et al., 1980) indicate a strong structural homology about the heme sites among cytochromes *c'*. All cytochromes *c'* investigated thus far have thioether bonds between the heme vinyl substituents and cysteine residues of the protein. The site of covalent heme attachment is near the C terminus of each peptide with an amino acid sequence -C-X-X-C-H-, typical of *c*-type cytochromes. The spin states of the iron centers are, however, more complex and are atypical of *c*-type cytochromes. The electronic ground states of ferricytochromes *c'* have been studied intensively using a variety of spectroscopic techniques. These techniques include electron spin resonance (Maltempo, 1975), nuclear magnetic resonance (Emptage et al., 1981; La Mar et al., 1981), magnetic circular dichroism (Suzuki et al., 1988), optical circular dichroism (Rawlings et al., 1977), and resonance Raman spectroscopy (Strekas & Spiro, 1974; Kitagawa et al., 1977). These and other studies of model heme complexes (Reed et al., 1979) indicate that a quantum-mechanical admixture of $S = {}^5/_2$ and $S = {}^3/_2$ states is favored for the ferric spin state of *C. vinosum* cytochrome *c'* at physiological pH. In contrast, ferricytochromes *c'* from other bacterial sources may exist in a simple $S = {}^3/_2$ spin state (Moore et al., 1982). Although ferricytochromes *c'* from different species have been postulated as having slightly different electronic ground states, it is generally agreed that they are structurally similar, with a histidine proximal to the heme occupying the fifth coordination position of the iron ion. Thus, while cytochromes *c'* are generally diverse in amino acid sequence, the heme pocket region is more highly conserved. X-ray data suggest that this proximal imidazole is, unlike those observed for hemoglobin and myoglobin, solvent-exposed. The distal heme pocket differs from those of globins in having closely packed, hydrophobic amino acid residues about the distal heme surface. Further evidence of the relative inac-

cessibility of the sixth coordination site in cytochromes *c'* is found in reduced binding affinities of ferrous cytochrome *c'* for CO and CN^-, relative to those observed for the globins (CO) or *c*-type cytochromes (CN^-) (Kassner et al., 1985; Cusanovich & Gibson, 1973).

Equivalence of Hemes in c' Dimer. At the protein concentrations used in this study, the dimeric form of cytochrome *c'* is highly favored ($K_D < 10^{-7}$ M) (Doyle et al., 1986) for both oxidized and reduced species. Our high-frequency data are consistent with the presence of a single heme species at all pH values and both Fe oxidation states. The line widths of all the prominent modes are similar to those of homogeneous heme proteins (full widths at half-maximum of 9–12 cm^{-1}). Thus, it appears that the two hemes of the cytochrome *c'* dimer are equivalent.

Equilibrium Ferricytochrome c'. The high-frequency spectra obtained at pH 7 (type I) and pH 10 (type II) using Soret excitation frequencies (406–440 nm) corroborate previous observations of the anomalous spin-state behavior of the cytochromes *c'*. X-ray crystallographic data from a similar diheme, dimeric cytochrome *c'*, indicate that, at physiological pH, the sixth coordination position of the heme is unoccupied (Weber et al., 1981). This is probably due to the closely packed hydrophobic environment of the distal heme pocket and accounts, at least partially, for the relatively small equilibrium constant ($K \approx 10^4$ M^{-1}) observed for CN^- binding.

It is now generally accepted that the type I species can be accurately described as a quantum-mechanical admixture of spin ($S = {}^5/_2, {}^3/_2$) coupled via spin–orbit effects. Raman data from this study and earlier investigations (Steakas & Spiro, 1974; Kitagawa et al., 1977) confirm this hypothesis. The high-frequency spectrum of ferric cytochrome *c'* at pH 7.0 is not typical of either a high-spin or a low-spin ferric heme. In particular, the ligation state sensitive Raman mode, ν_3, occurs as a single band at a frequency (1502 cm^{-1}) intermediate between those observed for high (~1495 cm^{-1}) and low (~1505 cm^{-1}) spin heme species.

Spectral changes associated with the interconversion between type II and type I have been attributed to the protonation state of the N_δ1 of the histidine axial ligand (Weber, 1982). Deprotonation of the axial histidine is believed to increase ligand field strength and thus the relative occupation of the $d_{x^2-y^2}$ orbitals. Further increases in pH to produce the type III form result in a Raman spectrum consistent with the binding of a strong-field ligand. Previous studies (Strekas & Spiro, 1974; Kitagawa et al., 1977) have suggested a nitrogenous distal ligand such as histidine or lysine. The binding of a second histidine can be ruled out in this species based upon AA sequence data which locate only one histidine among the residues in the protein. X-ray crystallographic data, however, locate several lysine residues in the heme milieu. These are the most likely candidates for ligation to the heme in the type III species.

Equilibrium Ferrocytochrome c'. The high-frequency Raman spectrum of ferrocytochrome *c'* at pH 12 is generally consistent with those reported for reduced, *c*-type cytochromes. The positions of ν_4 (1358 cm^{-1}), ν_3 (1488 cm^{-1}), and ν_2 (1592 cm^{-1}) are indicative of the binding of a sixth ligand to the heme iron and the formation of a low-spin electronic ground state. As in the spectrum of ferricytochrome *c'* at pH 12, there is evidence of a reduction in electron density of the porphyrin e_g* molecular orbitals by the 7 cm^{-1} shift in ν_4 to higher frequency. Thus, while the axial ligands have π acid characteristics, they are significantly weaker than ligands such as CO or CN^- which shift ν_4 by 10–13 cm^{-1}. Furthermore, it is expected that π back-bonding should be larger for the ferrous iron due to its smaller net charge. We therefore conclude that the endogenous sixth ligand which coordinates to the heme at pH 12 is a σ donor, possibly a lysine residue.

The high-frequency Raman spectrum of ferrocytochrome *c'* at pH 7 (type a) is also clearly anomalous compared to those of other *c*-type cytochromes under similar solution conditions. These differences are most certainly due to a dramatic alteration in heme pocket structure, resulting in a 5-coordinate, high-spin heme. Thus, it is appropriate to compare spectra of ferrocytochrome *c'* at pH 7 to those of deoxyhemoglobin and a novel ligand binding heme protein also isolated from *C. vinosum* and previously characterized in our laboratory (Ondrias et al., 1984; Gaul et al., 1987). Raman spectra of this novel heme protein, *Chromatium* high-spin protein (CHP), indicate that it contains a high-spin, 5-coordinate heme bound via thioether bonds to the protein.

The core size of the hemes in cytochrome *c'* is larger than that of deoxy-Hb as evidenced by the lower values observed for ν_4, ν_3, and ν_{10} (see Table II). This observation suggests that the iron ion is less out of the heme plane in cytochrome *c'* than it is in deoxy-Hb and is consistent with previous Raman data (Strekas & Spiro, 1974) as well as more recent X-ray and EXAFS data (Korszun et al., 1989) which report the iron out-of-plane distance in reduced cytochromes *c'* to be approximately 0.30 Å.

Our high-frequency data from the type *a* species do, however, compare favorably to spectra of the high-spin, 5-coordinate heme in CHP (see Table II). The intensities of ν_2 (~1580 cm^{-1}) and ν_{11} (~1540 cm^{-1}) in the spectrum of cytochrome *c'* at pH 7 are quite anomalous and most likely result from environmental perturbation of the heme. These modes are primarily associated with C_b–C_b stretching of the heme pyrrole and are, therefore, expected to be quite sensitive to perturbations at the heme periphery. These perturbations may be a direct result of the covalent bonding of heme vinyls and cysteinyl residues or to steric interactions between the heme periphery and the local heme pocket. Transient Raman results (see below) suggest that steric interactions are the most likely explanation.

Cytochromes *c'*, like many other heme proteins, are believed to have an imidazole from a proximal histidine as the fifth ligand to the heme iron. Because an imidazole is trans to the physiologically relevant ligand binding site in enzymes such as hemoglobins, myoglobins, oxidases, and peroxidases, its role in distal ligand affinity and reactivity has been the subject of much inquiry. In particular, the frequency of ν_{Fe-His} has been found to be useful in assessing the protonation state and geometry of the proximal histidine (Ondrias et al., 1982; Kitagawa, 1987). Thus, the relative position of this mode, as well as the low-frequency porphyrin modes, can be extremely useful in evaluating the heme environment. Iron–histidine modes for pentacoordinate heme proteins have been observed with a range of Raman shift frequencies between approximately 200 and 250 cm^{-1} (Spiro, 1983; Babcock, 1980; Kitagawa, 1987). Our results indicate that ν_{Fe-His} for dimeric ferrocytochrome *c'* occurs at ~231 cm^{-1}. This assignment is based upon analogies to other heme proteins and the absence of this mode in the hexacoordinate forms of the enzyme [i.e., the type n (pH 12) and CO-ligated species]. Also, in the CO-ligated samples, this mode gains intensity upon photolysis of CO, which generates the pentacoordinate monomer of the complex in the time scale studied. Clearly, ^{57}Fe isotopic substitution experiments are required to make a definitive assignment.

The positions of ν_{Fe-His} for ferrocytochrome *c'* are intermediate between those reported for the globins (~220 cm^{-1}) and peroxidases (~240 cm^{-1}). This probably reflects differences in the tertiary structure of the protein in the proximal region of the heme. Specifically, the solvent exposure of this region would prevent hydrogen bonding of any proximal amino acid residue, such as a carboxylate from a glutamic acid, to the $N_{\delta 1}$ proton of the histidyl imidazole. Hydrogen bonding has been shown to significantly alter the Fe–His position in both model compounds and heme proteins (Kitagawa, 1987). Finally, our data indicate that ν_{Fe-His} for the dimer does not vary significantly from that transiently observed in the monomer (see below). We speculate that the proximal side of the heme is unaffected by dissociation of the dimer and thus it is likely that the proximal region of the monomer is also solvent-exposed.

Heme low-frequency modes in ferricytochrome *c'* are, however, affected by pH changes. As previously noted, the low-frequency Raman spectrum (<600 cm^{-1}) is dominated by modes involving porphyrin deformation and by substituent bending modes at the C_b pyrrole carbons (Spiro, 1983). In cytochromes *c'*, the type n (pH 12.0) transition is associated with the binding of a relatively strong-field ligand and movement of the heme iron into the plane of the porphyrin. This transition to a more highly symmetric porphyrin may account for the increased intensity of heme modes observed using Soret excitation. The low-frequency spectrum of the planar (type n) form compares well to that observed for several *c*-type cytochromes which may have similar heme symmetry.

The low-frequency spectrum of the type a form does not compare favorably with that obtained for other 5-coordinate heme proteins such as hemoglobin or myoglobin. This is no doubt due to differences in the peripheral substituents at the C_b position of the macrocycle as well as differences in the distal protein environment.

Equilibrium CO-Ligated Species. The CO-bound forms at physiological and alkaline pH were prepared and investigated by using resonance Raman and infrared spectroscopies in order to further study heme pocket structure and dynamics. Cytochrome *c'* has been shown to possess a unique protein structure in the proximal and distal regions of the heme. Further evidence of the coupling between ligand binding and protein tertiary structure can be found in the large effect produced by CO binding upon the protein monomer–dimer equilibrium (Doyle et al., 1986). The high-frequency spectra of the CO-ligated cytochrome *c'* obtained by using Soret excitation at both pH 7 and pH 12 are remarkable in their similarities and correlate quite well to the high-frequency spectra of CO-ligated Hb and Mb (see Table II). This behavior contrasts with the pH sensitivity demonstrated by ferrocytochrome *c'* in the absence of CO and suggests that the heme geometry of the ligated protein is relatively insensitive to pH-induced changes in protein structure.

The geometry of CO binding is, by large, dictated by the distal heme pocket environment. Additionally, studies of equilibrium heme–CO model complexes and CO-bound heme proteins demonstrated that the Fe–C–O and C=O vibrational modes are quite sensitive to both electronic and geometric factors (Yu et al., 1983; Evangelista-Kirkup et al., 1986; Uno et al., 1987; Li & Spiro, 1988). The Fe–C stretching mode is especially variable, exhibiting frequencies ranging from 464 to 537 cm^{-1}. Its position can be correlated to changes in Fe $d_\pi \rightarrow CO\pi^*$ back-donation and to kinematic and electronic effects produced by distortions from a linear Fe–C–O geometry [see Li and Spiro (1988) for a complete discussion]. Heme proteins exhibit a variety of Fe–C and C=O stretching frequencies. While the relative contributions of back-bonding and Fe–C–O geometry to ν_{Fe-C} and $\nu_{C=O}$ variations are model-dependent, it is clear that these modes are sensitive indicators of both proximal and distal heme pocket configurations.

The behavior of $\nu_{C=O}$ and ν_{Fe-C} for cytochrome *c'* indicates that the protein possesses a distinctive heme pocket. The positions of $\nu_{C=O}$ (1978 and 1972 cm^{-1} for pH 7 and pH 12, respectively) are considerably higher than those reported for other heme proteins [see Table I and Li and Spiro (1988)], while the frequencies observed for ν_{Fe-C} are anomalously low. A higher energy C–O stretch indicates a stronger C–O bond and is consistent with a reduction in back-donation of electron density from the metal d_π orbitals to the π^* orbital of the carbonyl ligand.

IR and Raman studies of metal carbonyl compounds have demonstrated that, as the extent of back-bonding from the metal to the carbonyl decreases, the metal–carbon bond becomes weaker and the C–O bond becomes stronger (Braterman, 1975). Indeed, an inverse linear relationship between ν_{Fe-C} and ν_{CO} has been found for a number of metal carbonyl compounds and heme proteins (Li & Spiro, 1988; Uno et al., 1987). A plot of the observed ν_{Fe-C} vs ν_{CO} for a variety of heme proteins as well as metalloporphyrin–CO compounds can be accurately fit by a straight line given by $\nu_{Fe-C} = 1935 - 0.73\nu_{CO}$. Significant deviations from this line are interpreted as resulting from a trans effect upon the carbonyl by variations in the σ donor ability of the proximal imidazole ligand (Li & Spiro, 1988). The negative correlation in bond strength between ν_{Fe-C} and ν_{CO} is attributed to changes in $Fe(d_\pi)$–$CO(\pi^*)$ back-bonding due to a distortion of Fe–C–O geometry from the electronically preferred linear, perpendicular configuration.

The excellent quantitative fit of our data [calculated ν_{Fe-C}(pH 7) and ν_{Fe-C}(pH 12) of 491 and 495 cm^{-1}, respectively] to this negative correlation strongly suggests that pH-induced changes in $\nu_{C=O}$ and ν_{Fe-C} do not result from variations in the donor ability of the proximal histidine. Thus, distal pocket geometry or polarity could be responsible for the anomalous $\nu_{C=O}$ and ν_{Fe-C} positions in cytochrome *c'*. Distortions from linear perpendicular binding may involve Fe–C–O tilting or bending and would be consistent with the presumed crowded, nonpolar distal pocket of cytochrome *c'*. Interestingly, Nagai and co-workers (Nagai et al., 1987) have shown that replacement of the distal histidine in hemoglobin β chains with nonpolar residues (valine and glycine) produces ν_{CO} and ν_{Fe-C} positions of ~1970 and 493 cm^{-1}, respectively. These results suggest that the polarity of the distal heme pocket may also strongly influence CO bonding.

A closer examination of both ν_{Fe-C} and $\nu_{C=O}$ reveals strong evidence for inhomogeneity within the distal heme pocket of cytochrome *c'*. The pH-dependent line shape of $\nu_{C=O}$ is particularly broad (full width at half-height ≈25) cm^{-1} and asymmetric. It can be deconvoluted into four components (1984, 1979, 1966, and 1954 cm^{-1}) at neutral pH (see Figure 8). We conclude that the pH dependence in the composite band results from interconversions of the bands at 1985 and 1967 cm^{-1}. Other bands are not significantly affected by pH changes. This conformational heterogeneity is corroborated by the slightly broader line width ($\Gamma \approx 20$ cm^{-1}) of ν_{Fe-C} relative to those of most other heme proteins ($\Gamma \approx 15$ cm^{-1}). The multiple bands observed for the C–O stretching mode indicate the presence of several different ligand conformations within the cytochrome *c'* distal heme pocket. Moreover, all of the major conformers are significantly distorted from a

linear, perpendicular geometry since they exhibit $\nu_{C=O} > 1960$ cm^{-1} and $\nu_{Fe-C} < 500$ cm^{-1}.

CO Photolysis and Transient Spectra. Transient resonance Raman spectroscopy has recently been shown to be an informative probe of the heme pocket dynamics accompanying ligand binding in hemoglobins and other heme-containing proteins. Photolysis of CO from the heme active sites is very efficient ($\phi \approx 1.0$) and results in the creation of a high-spin, 5-coordinate heme in less than a picosecond after the absorption of a photon (Rousseau & Friedman, 1988; Findsen et al., 1985; Dasgupta et al., 1985; Petrich et al., 1988; Friedman, 1985). Resonance Raman spectra of the heme generated immediately after (<10 ns) photolysis reveal the interactions between the heme and metastable configurations of the unrelaxed heme pocket. They can also be used to assess the extent of prompt geminate ligand recombination. The transient Raman spectra obtained in this study show that the heme pocket dynamics subsequent to CO photolysis from cytochrome *c'* are quite dependent upon pH-induced differences in protein tertiary structure.

Even under saturating excitation conditions (>10 photons per heme·CO) which ensure complete photolysis of CO, the transient Raman spectra exhibit modes arising from CO-bound heme sites. This is most evident in the behavior of ν_4. The substantial intensity of this mode at $\sim$1370 cm^{-1} in the 10-ns transient spectra indicates that significant heme–CO geminate recombination occurs within the laser pulse width. Previous studies of CO photolysis from Hb and Mb (Rousseau & Friedman, 1988; Scott & Friedman, 1984) have concluded that the escape of the photolyzed ligand from the distal heme pocket is a determining factor in the amount of geminate (as opposed to bimolecular) heme–CO recombination. Ligand escape is, in turn, critically dependent upon protein tertiary structure. For instance, Mb exhibits markedly less geminate recombination than R-state hemoglobins (Rousseau & Friedman, 1988; Friedman et al., 1985b), presumably because it possesses a more "open" distal heme pocket. We speculate that the net photolysis yield of cytochrome *c'* is controlled by similar factors. The extent of geminate recombination of cytochrome *c'* (at any pH) greatly exceeds that of even R-state hemoglobin (Friedman et al., 1985a,b). This behavior is consistent with a tightly packed, hydrophobic distal pocket which affects even the bound heme–CO geometry. The distal pocket tertiary structure also apparently inhibits diffusion of the photolyzed CO away from the heme and thus facilitates geminate recombination. At pH 12, the distal heme pocket has an altered tertiary structure which favors binding of a protein residue to the heme. This presumably results in an even more "restricted" distal heme pocket and further increases the probability of heme·CO recombination.

The spectra of the heme sites that do not geminately recombine are extremely informative concerning heme–protein dynamics in cytochrome *c'*. They reveal that, within 10 ns of CO photolysis, the heme pocket is not in its equilibrium configuration. The transient species created by CO photolysis are distinctive (relative to the well-studied Hb photolytic transients) and pH dependent.

At pH 7.0, CO photolysis produces a high-spin species which is clearly different from the equilibrium ferrous species. It exhibits an intense ν_2 band at $\sim$1581 cm^{-1} and a reduced intensity for ν_{11} at $\sim$1540 cm^{-1} (see Figure 3). In this respect, the photolytic transient more closely resembles a "typical" high-spin 5-coordinate ferrous heme than the equilibrium species. Transient changes in these modes cannot be due to core size differences or distortions of heme planarity since ν_3 and ν_{10} would also be affected (Spiro, 1983; Alden et al., 1989). Moreover, they cannot arise from the covalent bonding of the heme vinyl groups because this remains unaltered in the photolytic transient species. We conclude that steric perturbations at the heme periphery are present in the equilibrium species but absent in the photolytic transients. Since the photolytic transient is a monomeric protein species, it is inviting to speculate that protein dimerization (which occurs on a time scale much longer than 10 ns) is responsible for the anomalous properties of the equilibrium species.

Curiously, the position of ν_{Fe-His} in the 10-ns photolytic transient is the same as in the equilibrium species. CO photolysis from hemoglobins results in systematic, time-dependent changes in these modes which have been interpreted in terms of the relaxation of the proximal heme pocket and its subsequent effects upon Fe–His bonding and heme electronics (Rousseau & Friedman, 1988). Similar proximal heme pocket dynamics are apparently absent in the photolytic transients of cytochrome *c'*.

Cytochrome *c'* also exhibits interesting photodynamics at pH 12.0. The positions of ν_3 (1469 cm^{-1}) and ν_2 ($\sim$1580 cm^{-1}) for the photolytic transient are clearly indicative of a high-spin species. Thus, it is apparent that the sixth ligand present in the equilibrium species does not bind to the photolyzed heme on a 10-ns time scale. Evidently, this process requires some rearrangement of distal heme pocket geometry. Similarities exist in the high-frequency spectra of photolyzed cytochrome *c'* at pH 12.0 and the equilibrium unligated pH 7.0 species (see Figures 2 and 3). However, the behavior of ν_4 and ν_{Fe-His} makes it clear that these species are not equivalent. The absence of an intense ν_{Fe-His} in the spectra of photolyzed *c'* at pH 12.0 is quite anomalous relative to other high-spin heme–imidazole species and definitely suggests an unusual heme–histidine geometry.

The relative intensities of the Fe–His modes of 6-coordinate, planar heme imidazole species are generally much lower than those of 5-coordinate, nonplanar species (Spiro, 1983). This presumably results from increased coupling of the heme π–π^* system and the Fe–His stretching mode in the nonplanar species (Bangcharoenpaurpong et al., 1984). We speculate that the reduced Fe–His intensity of the cytochrome *c'* phototransient is indicative of a largely in-plane Fe atom in that species. This scenario is also consistent with the enhanced geminate recombination rate of the pH 12 species. Much of the barrier to ligand recombination undoubtedly involves motion of the iron into the porphyrin plane. If, in fact, the iron does not move out of the heme plane subsequent to CO photolysis, the geminate recombination rate should be enhanced.

Conclusions

The data obtained in this study reveal the influence of the heme pocket tertiary structure upon the equilibrium and photolyzed heme active sites of cytochrome *c'*. Dimerization of the protein yields equivalent heme sites which are unique from those of other cytochromes. The sensitivity of the equilibrium heme pocket to pH variations is evident in the heme vibrational spectra of both ferric and ferrous species.

The ligand binding properties of cytochrome *c'* are also anomalous. Resonance Raman and infrared spectra of CO-bound cytochrome *c'* show that the close-packed distal heme pocket significantly constrains the heme–CO geometry. The net yield of CO photolysis and the heme pocket dynamics subsequent to photolysis are quite pH dependent. The high yield for geminate recombination (at all pH values) indicates that the escape of the photolyzed CO from the distal pocket

is inhibited. The reorganization dynamics of the heme pocket in the phototransient species are quite distinct from those of other heme proteins.

Registry No. CO, 630-08-0; cytochrome *c'*, 9035-41-0; heme, 14875-96-8.

REFERENCES

Alden, R. G., Crawford, B. A., Doolen, R., Ondrias, M. R., & Shelnutt, J. A. (1989) *J. Am. Chem. Soc. 111*, 2070–2073.

Ambler, R. P., Bartsch, R. G., Daniel, M., Kamen, M. D., McLellen, L., Meyer, T. E., & Beeumen, J. V. (1981) *Proc. Natl. Acad. Sci. U.S.A. 78*, 6854–6857.

Babcock, G. T. (1988) in *Biological Applications of Raman Spectroscopy* (Spiro, T. G., Ed.) Vol. III, pp 294–346, Wiley, New York.

Bangcharoenpaurpong, O., Schomacker, K. T., & Champion, P. M. (1984) *J. Am. Chem. Soc. 106*, 5688–5698.

Bartsch, R. G. (1971) *Methods Enzymol. 23*, 344–363.

Bartsch, R. G. (1978) in *The Photosynthetic Bacteria* (Clayton, R. K., & Sistrom, W. R., Eds.) pp 249–280, Plenum, New York.

Choi, S., & Spiro, T. G. (1983) *J. Am. Chem. Soc. 105*, 3683–3692.

Cusanovich, M. A. (1971) *Biochim. Biophys. Acta 236*, 238–241.

Cusanovich, M. A., & Gibson, Q. H. (1973) *J. Biol. Chem. 248*, 822–834.

Dasgupta, S., Spiro, T. G., Johnson, C. K., Dalickas, G. A., & Hochstrasser, R. (1985) *Biochemistry 24*, 5295–5299.

Dasgupta, S., et al. (1989) *J. Biol. Chem. 264*, 654–662.

Doyle, M. L., Gill, S. J., & Cusanovich, M. A. (1986) *Biochemistry 25*, 2509–2516.

Emptage, M. H., Xavier, A. V., Wood, J. M., Alsaadi, B. M., Moore, G. R., Pitt, R. C., Williams, R. J. P., Ambler, R. P., & Bartsch, R. G. (1981) *Biochemistry 20*, 58–64.

Evangelista-Kirkup, R., Smulevich, G., & Spiro, T. G. (1986) *Biochemistry 25*, 4420–4425.

Felton, R. H., & Yu, N.-T. (1983) in *The Porphyrins*, Vol. III, pp 347–393, Academic Press, New York.

Findsen, E. W., Friedman, J. M., Ondrias, M. R., & Simon, S. R. (1985) *Science 229*, 661–665.

Findsen, E. W., Friedman, J. M., & Ondrias, M. R. (1988) *Biochemistry 27*, 8719–8724.

Friedman, J. M. (1985) *Science (Washington, D.C.) 228*, 1273–1280.

Friedman, J. M., et al. (1982) *Science (Washington, D.C.) 218*, 1244–1246.

Friedman, J. M., et al. (1985) *Science 229*, 187.

Gaul, D. F., Ondrias, M. R., Findsen, E. W., Palmer, G., Olson, J. S., Davidson, M. W., & Knaff, D. B. (1987) *J. Biol. Chem. 262*, 1144–1147.

Imai, Y., Imai, K., Sato, R., & Horio, T. (1969) *J. Biochem. 65*, 225–237.

Kassner, R. J., Kykta, M. G., & Cusanovich, M. A. (1985) *Biochim. Biophys. Acta 831*, 155–158.

Kennel, S. J., Meyer, T. E., Kamen, M. D., & Bartsch, R. G. (1972) *Proc. Natl. Acad. Sci. U.S.A. 69*, 3432–3435.

Kitagawa, T. (1988) in *Biological Applications of Raman Spectroscopy* (Spiro, T. G., Ed.) Vol. III, pp 97–131, Wiley, New York.

Kitagawa, T., Ozaki, Y., Kyogoku, Y., & Horio, T. (1977) *Biochim. Biophys. Acta 495*, 1–11.

Korszun, Z. R., Bunker, G., Khalid, S., Scheidt, W. R., Cusanovich, M. A., & Meyer, T. E. (1989) *Biochemistry 28*, 1513–1517.

LaMar, G. N., Jackson, J. T., & Bartsch, R. G. (1981) *J. Am. Chem. Soc. 103*, 4405–4410.

Li, X.-Y., & Spiro, T. G. (1988) *J. Am. Chem. Soc. 111*, 6024–6033.

Maltempo, M. M. (1975) *Biochim. Biophys. Acta 379*, 95–102.

Maltempo, M. M., Moss, T. H., & Cusanovich, M. A. (1974) *Biochim. Biophys. Acta 342*, 290–305.

Meyer, T. E., & Kamen, M. D. (1982) *Adv. Protein Chem. 35*, 105–212.

Moore, G. R., McClune, G. J., Clayden, N. J., Williams, R. J. P., Akaadi, B. M., Angström, Ambler, R. P., Beeumen, J. V., Tempst, P., Bartsch, R. G., Meyer, T. E., & Kamen, M. D. (1982) *Eur. J. Biochem. 123*, 73–80.

Nagai, K., Luisi, B., Shih, D., Miyazaki, G., Imai, K., Payart, C., DeYoung, A., Kwiatkowsky, L., Noble, R. W., Lin, S.-H., & Yu, N.-T. (1987) *Nature (London) 329*, 888.

Ondrias, M. R., Rousseau, D. L., Shelnutt J. A., & Simon, S. R. (1982) *Biochemistry 21*, 1740–1747.

Ondrias, M. R., Findsen, E. W., Gaul, D. F., & Knaff, D. B. (1984) *Biochim. Biophys. Acta 788*, 87–97.

Petrich, J. W., Poyart, C., & Martin, J. L. (1988) *Biochemistry 27*, 4049–4057.

Rawlings, J., Stephens, P. J., Nafie, L. A., & Kamen, M. D. (1977) *Biochemistry 16*, 1725–1729.

Reed, C. A., Mashiko, T., Bentley, S. P., Kastner, M. E., Scherdt, W. R., Spartalian, K., & Lang, G. (1979) *J. Am. Chem. Soc. 101*, 2948–2958.

Rousseau, D. L., & Friedman, J. M. (1988) in *Biological Applications of Raman Spectroscopy* (Spiro, T. G., Ed.) Wiley, New York.

Rubinow, S. C., & Kassner, R. J. (1984) *Biochemistry 23*, 2590–2595.

Scott, T. W., & Friedman, J. M. (1984) *J. Am. Chem. Soc. 106*, 5677–5687.

Shimada, H., & Caughey, W. S. (1982) *J. Biol. Chem. 257*, 11893–11900.

Spiro, T. G. (1983) in *Iron Porphyrins* (Lever, A. B. P., & Gray, H. B., Eds.) Part II, pp 91–159, Addison-Wesley Publishing Co., Reading, Ma.

Strekas, T. C., & Spiro, T. G. (1974) *Biochim. Biophys. Acta 351*, 237–245.

Suzuki, S., Nakahara, A., Tetsuhiko, Y., Iwsaki, T., Shidara, S., & Matsubara, T. (1988) *Inorg. Chem. Acta*, 227–233.

Uno, T., Nishimura, Y., Tsuboi, M., Makino, R., Iizuka, T., & Ishimura, Y. (1987) *J. Biol. Chem. 262*, 4549–4556.

Weber, P. C. (1982) *Biochemistry 21*, 5110–5119.

Weber, P. C., Bartsch, R. G., Cusanovich, M. A., Hamlin, R. C., Howard, A., Jordan S. R., Kamen, M. D., Meyer, T. E., Weatherford, D. W., Xuong, N., & Salemme, F. R. (1980) *Nature 286*, 302–304.

Weber, P. C., Howard, A., Xuong, N. H., & Salemme, F. R. (1981) *J. Mol. Biol. 153*, 399–424.

Yu, N.-T., & Kerr, E. A. (1988) in *Biological Applications of Raman Scattering* (Spiro, T. G., Ed.) pp 39–95, Wiley, New York.

Yu, N.-T., Kerr, E. A., Ward, B., & Chany, C. (1983) *Biochemistry 22*, 4534–4540.